# DYNAMIC EFFECTS AND INFORMATION QUANTIFIERS OF STATISTICAL MEMORY OF MEG'S SIGNALS AT PHOTOSENSITIVE EPILEPSY

R. M. Yulmetyev[1,2], E. V. Khusaenova[1,2] and D. G. Yulmetyeva[1,2]

[1] Department of Physics, Kazan State University, Kremlevskaya Street, 18 Kazan, 420008 Russia
[2] Department of Physics
Tatar State University of Pedagogical and Humanities Sciences
Tatarstan Street, 2 Kazan, 420021, Russia

P. Hänggi

Department of Physics, University of Augsburg
Universitätsstrasse 1, D-86135 Augsburg, Germany

S. Shimojo

Division of Biology, CalTech, Pasadena, CA 91125, USA

K. Watanabe

Research Group for Decision Making
Research Center for Advanced Science and Technology
University of Tokyo, Tokyo, 153-8904, Japan

J. Bhattacharya

Department of Psychology, Goldsmits College
University of London, New Cross, London, SE14 6NW, UK

(Communicated by Ying-Cheng Lai)

Abstract. The time series analysis of magnetoencephalographic (MEG) signals is very important both for basic brain research and for medical diagnosis and treatment. Here we discuss the crucial role of statistical memory effects (ME) in human brain functioning with photosensitive epilepsy (PSE). We study two independent statistical memory quantifiers that reflect the dynamical characteristics of neuromagnetic brain responses on a flickering stimulus of different colored combinations from a group of control subjects, which are contrasted with those from a patient with PSE. We analyze the frequency dependence of two memory measures for the neuromagnetic signals. The strong memory and the accompanying transition to a regular and robust regime of the signals' chaotic behavior in the separate areas are characteristic for a patient with PSE. This particularly interesting observation most likely identifies the regions of the protective mechanism in a human organism against occurrence of PSE.

2000 *Mathematics Subject Classification.* Primary: 94A17, 92C55; Secondary: 92C50, 60K40.
*Key words and phrases.* human brain, statistical memory, information quantifiers, stochastic processes, photosensitive epilepsy.
The first author is supported by the Grants of RFBR 08-02-00123a and Ministry of Education and Science of Russian Federation No. 2. 1. 1. 741.

1. **Introduction.** The statistical characteristics of brain electromagnetic signals have generated considerable interest, and many studies have been performed recently in order to understand the origin and the role as well as the dynamics of the neural activity [16, 3, 26, 12]. Studies of MEG as well as electroencephalogram (EEG) provide unique insights into the dynamic behavior of the human brain, as they are able to follow changes in neural activity on a millisecond time scale [11]. The physical processes of neural physiological activity can be registered with noninvasive measurement techniques on the basis of EEG and MEG. These macroscopic electrophysiological techniques permit the tracing of the time evolution of neural population activation with millisecond temporal resolution. Neural electromagnetic responses are handled also physical processes that relate to electric and magnetic fields in other complex systems.

The observed neuronal behavior at the surface of the human cortex measured by MEG or EEG is characterized by the regions of relatively random behavior of electric and magnetic signals that change according to the state of the subject and the position in the head. The responses to individual stimuli or affecting processes typically require the specialized methods and models of signal processing.

Growing attention has recently been paid to the study of statistical ME in random processes that originate from the brain signals by means of nonequilibrium statistical physics. The understanding of the crucial role of memory in chaotic dynamics of complex systems has its roots [17] in kinetic and relaxation processes in gases [7] and plasma [1], condensed matter physics (liquids [22], solids [15], and superconductivity [9]), astrophysics [23], nuclear physics [8], quantum [30] and classical [6] physics, etc. Nowadays, we can make use of a variety of statistical methods for the analysis of ME in diverse physical systems. Typical similar schemes are Zwanzig-Mori's kinetic equations [29], generalized master equations and corresponding statistical quantifiers [10], Lee's recurrence relation method [2], the generalized Langevin equation (GLE) [14], etc.

Here we show that statistical ME play an important role in the functioning of the human brain. Particularly, it can mean that the appearance of strong ME (and respectively, large memory times-scales) in the stochastic dynamics of neuromagnetic signals can specify the pathological (or catastrophic) breaking of dynamic states of the healthy human brain. As an example, we will show here that the occurrence of strong ME (and respectively, large time scales of memory) in the stochastic behavior of human brain neuromagnetic responses recorded by MEG is accomplished by the generation and the existence of PSE.

Let's remember that the correlation function represents the quantitative measure for the compact description of the wide classes of correlation in complex systems. The correlation function in statistical mechanics is a measure of order in the random system. It shows the way microscopic variables at different positions are correlated.

ME in stochastic processes also reveal through correlations. ME appear at a more detailed level of statistical description of correlation by the hierarchical manner. ME reflect the complicated or hidden character of the creation, the propagation and the decay of correlation. ME are produced by inherent interactions and statistical after effects in complex systems. For statistical systems ME are induced by contracted description of the evolution of the dynamic variables by the use of memory functions (MF). MF describe the mutual interrelations between the rates of change of random variables on different levels of the statistical description.

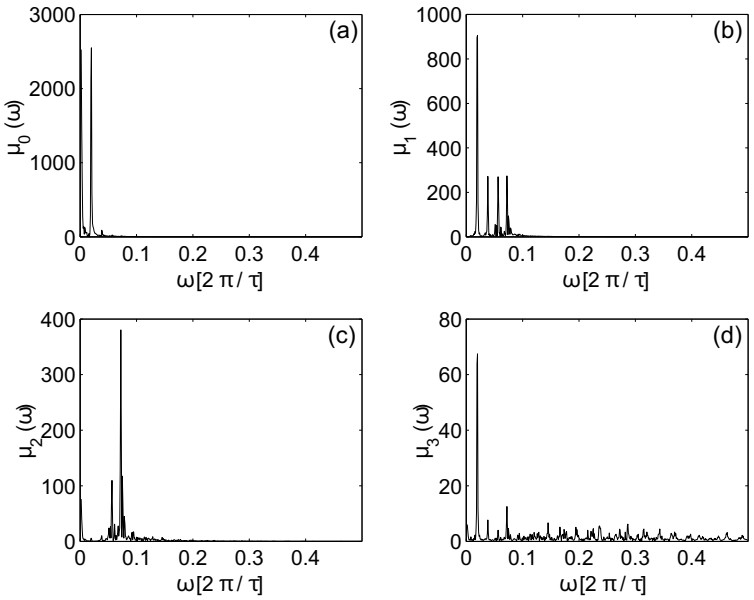


FIGURE 1. Frequency power spectra $\mu_i(\omega), i = 0, 1, 2$ and 3 for the healthy subject No. 7 (sensor No.10) (an R/B combination of the light stimulus) in linear scale for the set of four time correlation functions: a) for the initial TCF $a(t)$; b) for the first order MF $M_1(t)$; c) for the second order MF $M_2(t)$; d) for the third order MF $M_3(t)$.

The role of memory has its roots in the natural sciences since 1906, when the famous Russian mathematician Markov wrote his first paper on the theory of Markov Random Processes. The theory is based on the notion of the instant loss of memory from the prehistory (memoryless property) of random processes. From the physical point of view the time-scales of correlation and memory cannot be treated as arbitrary. Therefore one can introduce some statistical quantifiers for the quantitative comparison of these time-scales. They are dimensionless and possess the statistical spectra on different levels of the statistical description. As is conventional in probability theory and statistics, correlation (also so called correlation coefficient), means the strength and direction of a linear relationship between two random variables. In a general sense, correlation or co-relation reflects the deviation of two (or more) variables from independence, although correlation does not imply causation. In this broad sense there are some quantifiers that can measure degrees of correlation and ME, suited to the nature of data.

It is necessary to remember, that from the beginning, the statistical quantifiers of memory in time series for physiological systems that have been studied in EEG and MEG signals, both of healthy subjects and patients (including epilepsy patients), [27] were based on detrended-fluctuation analysis (DFA) [20].

2. **Memory functions formalism for discrete time series.** One of the powerful tools for the quantitative description of the statistical ME of random processes in the physiological data is the use of Zwanzig-Mori's kinetic equations and the MF

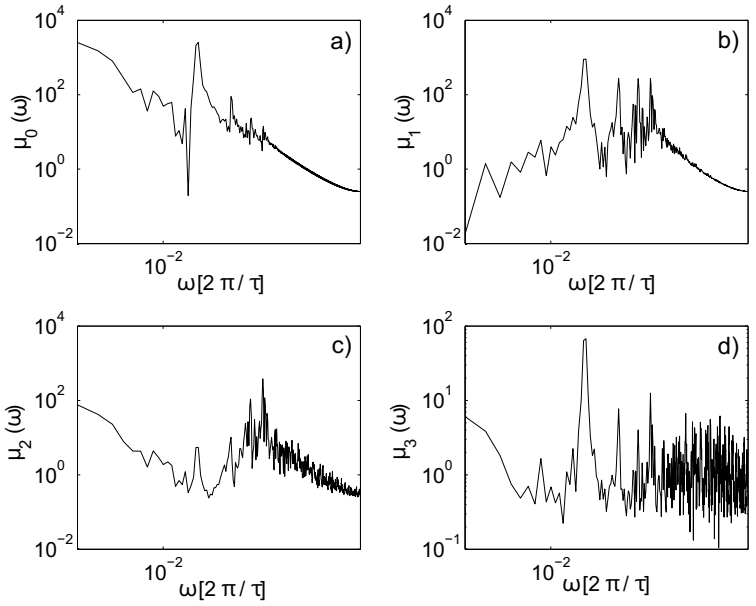


FIGURE 2. Frequency power spectra $\mu_i(\omega), i = 0, 1, 2$ and 3 for the healthy subject No. 7 (sensor No.10) (an R/B combination of the light stimulus) in double log-log scale. All designations same, as well as in Figure 1. One can notice multifractal behavior spectra of $\mu_i(\omega)$ for $i = 0$ and 2 with different behavior on the high and superlow frequencies.

formalism. By the use of arguments from [18] one can find the chain of interrelated finite-difference kinetic equations for the discrete time correlation function (TCF) $a(t) \equiv M_0(t) = \langle \delta x(t) \delta x(0) \rangle / \langle \delta x^2(0) \rangle$ of the fluctuation $\delta x(t) = x(t) - \langle x(t) \rangle$. Here $x(t) = (x_1; x_2; ...; x_N)$ is a random discrete-time process, i.e., $x_j = x(t_j)$, $t_j = j\tau$ and $\tau$ is a discretization time-step, $j = 1, 2, ...N$. Then this TCF is related to MF of the higher orders $M_i(t), i = 1, 2, ...$ through the set of interconnected equations. In accordance with this methodology [18] the discrete MF'-s $M_i(t), i = 1, 2, ...$ of $i$th order together with corresponding relaxation parameters quantifies the diverse ME. The whole set of MF'-s quantifies all the singularities of the ME for complex systems. For the discrete time series the whole set of functions $M_i(t)$ and relaxation parameters can be calculated directly from the experimental data [18].

The theory of discrete non-Markov stochastic processes [18] is based on the finite-difference representation of the kinetic Zwanzig-Mori's equations for condensed matter, which are well known in the statistical physics of nonequilibrium processes. The theory is also widely used in analyzing complex biological and physiological systems. Dynamic, kinetic, and relaxation parameters provided by this theory contain detailed information on a wide range of parameters and properties of complex systems.

Let's describe a discrete time series $x_j$ of variable $X$:

$$X = \{x(T), x(T + \tau), x(T + 2\tau), ..., x(T + \tau N - \tau)\}. \quad (1)$$

Here $T$ is the time of the beginning of time series, $(N - 1)\tau$ is the total time of signal recording, and $\tau$ is the discretization time. The normalized initial TCF is

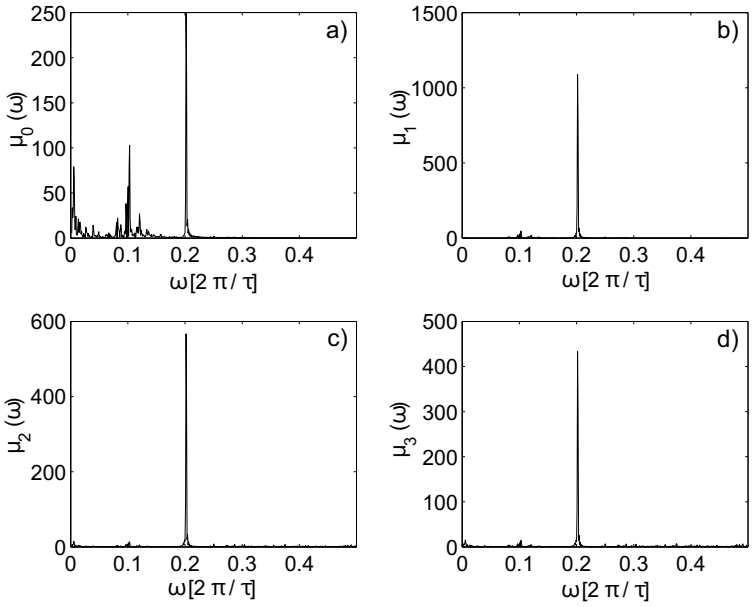


FIGURE 3. Frequency power spectra $\mu_i(\omega), i = 0, 1, 2$ and 3 for the patient with PSE (sensor No. 10) (an R/B combination of the light stimulus) in linear scale for the set of the four first TCF: a) for the initial TCF $a(t)$; b) for the first order MF $M_1(t)$; c) for the second order MF $M_2(t)$; d) for the third order MF $M_3(t)$. The sharp peak at the same frequency $\omega = 0.2 f.u.$ ($1 f.u. = 2\pi/\tau$) is typical for all spectra.

convenient for a description of the dynamics of the time correlation:

$$a(t) = \frac{1}{(N-m)\sigma^2} \sum_{j=0}^{N-1-m} \delta x_j \delta x_{j+m} =$$

$$= \frac{1}{(N-m)\sigma^2} \sum_{j=0}^{N-1-m} \delta x(T + j\tau)\delta x(T + (j+m)\tau), \qquad (2)$$

$$t = m\tau,\ 1 \le m \le N-1.$$

TCF depending on current $t = m\tau$ can be conveniently used to analyze dynamic properties of complex systems. TCF usage means that the developed method is true of complex systems, when correlation function exists. The mean value $\langle X \rangle$, fluctuations $\delta x_j$, absolute ($\sigma^2$), and relative ($\delta^2$) dispersion for a set of random variables (eq. 1) can be easily found by the following:

$$\langle X \rangle = \frac{1}{N} \sum_{j=0}^{N-1} x(T + j\tau),$$

$$x_j = x(T + j\tau), \delta x_j = x_j - \langle X \rangle,$$

$$\sigma^2 = \frac{1}{N} \sum_{j=0}^{N-1} \delta x_j, \delta^2 = \frac{\sigma^2}{\langle X \rangle^2}. \qquad (3)$$

The function $a(t)$ should satisfy the normalization condition and conditions of relaxation of time correlations:

$\lim_{t\to 0} a(t) = 1,\ \lim_{t\to\infty} a(t) = 0.$

On the basis of Zwanzig-Mori's technique of projection operators, it is possible to receive an interconnected chain of finite-difference equations of the non-Markov type for the initial TCF $a(t)$ and the normalized MF of the first order (and higher orders) in the following way:

$$\frac{\triangle a(t)}{\triangle t} = \lambda_1 a(t) - \tau\Lambda_1 \sum_{j=0}^{m-1} M_1(j\tau)\ a(t-j\tau). \tag{4}$$

Here, $\lambda_1$ is the eigenvalue and $\Lambda_1$ is the relaxation parameter of the Liouville's quasioperator $\hat{L}$. Function $M_1(j\tau)$ is normalized MF of the first order:

$$\lambda_1 = i\frac{\langle \mathbf{A}_k^0(0)\hat{L}\mathbf{A}_k^0(0)\rangle}{\langle|\mathbf{A}_k^0(0)|^2\rangle},\ \Lambda_1 = \frac{\langle \mathbf{A}_k^0(0)\hat{L}_{12}\hat{L}_{21}\mathbf{A}_k^0(0)\rangle}{\langle|\mathbf{A}_k^0(0)|^2\rangle},$$
$$M_1(j\tau) = \frac{\langle \mathbf{A}_k^0(0)\hat{L}_{12}(1+i\tau\hat{L}_{22})^j\mathbf{A}_k^0(0)\rangle}{\langle \mathbf{A}_k^0(0)\hat{L}_{12}\hat{L}_{21}\mathbf{A}_k^0(0)\rangle},\ M_1(0) = 1. \tag{5}$$

Gram-Schmidt orthogonalization procedure $\langle \mathbf{W}_n, \mathbf{W}_m\rangle = \delta_{n,m}\langle|\mathbf{W}_n|^2\rangle$, where $\delta_{n,m}$ is Kronecker's symbol, can be used to rewrite the dynamic orthogonal variables $\mathbf{W}_i$, i= 1, 2, 3... in a more compact form:

$$\mathbf{W}_0 = \mathbf{A}_k^0(0),\ \mathbf{W}_1 = (i\hat{L} - \lambda_1)\mathbf{W}_0,\ \mathbf{W}_2 = (i\hat{L} - \lambda_2)\mathbf{W}_1 - \Lambda_1\mathbf{W}_0, ...,$$
$$\mathbf{W}_n = (i\hat{L} - \lambda_n)\mathbf{W}_{n-1} - \Lambda_{n-1}\mathbf{W}_{n-2} - ... \ . \tag{6}$$

Then the eigenvalue $\lambda_1$ of Liouville's quasioperator and the relaxation parameter $\Lambda_1$ in equation (5) take the form of

$$\lambda_1 = i\frac{\langle \mathbf{W}_0\hat{L}\mathbf{W}_0\rangle}{\langle|\mathbf{W}_0|^2\rangle},\ \Lambda_1 = i\frac{\langle \mathbf{W}_0\hat{L}\mathbf{W}_1\rangle}{\langle|\mathbf{W}_0|^2\rangle}.$$

The normalized MF of the first order in equation (5) is rewritten as:

$$M_1(t) = \frac{\langle \mathbf{W}_1(1+i\tau\hat{L}_{22})^m\mathbf{W}_1\rangle}{\langle|\mathbf{W}_1(0)|^2\rangle}.$$

The finite-difference kinetic equation (4) combined with equations (5)-(8) represent the generalization of Zwanzig-Mori's kinetic theory, which is well known in statistical physics, for complex discrete non-Hamiltonian statistical systems. Within our method the analysis of dynamics of the statistical time series we use equation (4) as an object for subsequent theoretical analysis. In this connection we use the equations such as Zwanzig-Mori's for MF of the 2nd and higher orders. We use the algorithm, which was above described, for calculation the time dynamics $a(t)$, $M_1(t)$ and parameters $\lambda_1$, $\Lambda_1$. The dependence $a(t)$ and $M_1(t)$ is calculated on the basis of the experimental data independently of each other. At the same time we control the conformity of the calculated dependence $a(t)$, $M_1(t)$ and parameters $\lambda_1$, $\Lambda_1$ to the equation (4) (the precision of the conformity is $\sim 2-5\%$ for the cases described here). We use the dependence $a(t)$ and $M_1(t)$ to analyze the time dependence of MEG's signals. We also use these dependences to calculate the non-Markovity parameter which characterizes the strength of the statistical memory of the signals.

The earlier study shows that this parameter contains detailed information about the physiological state of a system.

3. **Information quantifiers of statistical memory.** In this paper we shall use the spectral dependence $\varepsilon_1(\nu)$ of the first point of the non-Markovian parameter:

$$\varepsilon_1(\nu) = \left\{ \frac{\mu_0(\nu)}{\mu_1(\nu)} \right\}^{\frac{1}{2}}, \tag{7}$$

which is determined by means of Fourier transformations $\mu_0(\nu)$, $\mu_1(\nu)$ of functions $a(t)$ and $M_1(t)$ respectively:

$$\mu_0(\nu) = \left| \Delta t \sum_{j=0}^{N-1} a(t_j) \cos(2\pi\nu t_j) \right|^2, \ \mu_1(\nu) = \left| \Delta t \sum_{j=0}^{N-1} M_1(t_j) \cos(2\pi\nu t_j) \right|^2.$$

Further we shall show that the application of the frequency-dependence $\varepsilon_1(\nu)$ and the values of this parameter on zero frequency

$$\varepsilon_1(\nu = 0) = \varepsilon_1(0) = \left\{ \frac{\mu_0(0)}{\mu_1(0)} \right\}^{\frac{1}{2}}, \tag{8}$$

allows for the introduction of quantitative estimations for various dynamic states in a patient with PSE. In particular, we shall show that the values of parameter $\varepsilon_1(0) \sim 10^1$ for the analyzed system are characteristic of stable physiological states (for the patient under treatment). The appearance of pathology in a system leads to a sharp decrease in this parameter, approximately by one order. Thus, we can compare quantitatively various dynamic states of the studied system by considering the change of the non-Markovity parameter.

To highlight the means of studying the role of ME in dynamics of complex systems we will follow the reasons of [18]. The characterizing of memory is based on the use the set of dimensionless statistical quantifiers which are capable of measuring the strength of memory that is inherent in the complex dynamics. First similar measure of memory is the measure $\varepsilon_i(\omega) = \{\mu_i(\omega)/\mu_{i+1}(\omega)\}^{1/2}$. Second measure is defined as $\delta_i(\omega) = |\tilde{M}_i'(\omega)/\ \tilde{M}_{i+1}'(\omega)|$. Here $\mu_i(\omega) = |\tilde{M}_i(\omega)|^2$ is a frequency power spectrum of the corresponding MF $M_i(t)$, $\tilde{M}_i'(\omega) = d\tilde{M}_i(\omega)/d\omega$ whereas $\tilde{M}_i(\omega)$ is a Fourier transform of the MF $M_i(t)$. Here $M_i(t) = \langle W_i(t)W_i(0)\rangle/\langle W_i^2(0)\rangle$ is a MF of i$th$ order, $W_i(t)$ is the corresponding dynamic orthogonal variable.

The aforementioned normalized MF of the i$th$ order is defined as follows:

$$M_i(t) = \frac{\langle \mathbf{W}_i(1 + i\tau\hat{L}_{22}^{(i)})^m \mathbf{W}_i\rangle}{\langle |\mathbf{W}_i(0)|^2\rangle},$$

where the variables $\mathbf{W}_i$ should be found by the Gram-Schmidt orthogonalization procedure (see, for example, equation (6)).

Discrete MF'-s $M_i(t)$ together with corresponding relaxation parameters quantify all diversity of the ME. The whole set of MF'-s quantifies all singularities of the ME for complex systems. For the discrete time series the whole of set of MF's $M_i(t)$ and relaxation parameters can be calculated directly from the experimental data. The measures $\varepsilon_i(\omega)$ are suitable for the quantification of the memory on a relative scale whereas the second set $\delta_i(\omega)$ proves to be useful for quantifying the amplification of the role of relative ME inherent to different complexity levels. Both measures provide the statistical criteria of the comparison between relaxation

time scales and memory time scales. In the case $\{\varepsilon, \delta\} >> 1$ one observes complex dynamics with the short-range temporal memory scales. For the limit $\{\varepsilon, \delta\} \to \infty$ these processes possess $\delta$-like memory. When $\{\varepsilon, \delta\} > 1$ one considers a situation with moderate (intermediate) memory strength. And the case with both $\varepsilon$, $\delta \sim 1$ matches up typically to the more regular and robust processes with the features of strong memory.

The characterization of memory is based on the set of dimensionless statistical quantifiers, which determine the ME in time evolution of complex systems. The set of parameters $\delta_i(\nu)$ proves useful for quantifying the amplification of relative ME occurring on different complexity levels. This measure provides the statistical criterion for the comparison of the relaxation time-scales and memory time-scales of the process under study. When parameter obeys $\delta \gg 1$, the complex system dynamics can be described by the short-range temporal memory scale. In the extreme case this process can be characterized by $\delta$-like memory with parameter $\delta \to \infty$. In the case of $\delta > 1$ one deals with a situation of moderate memory strength, and the case where $\delta \sim 1$ typically constitutes a more chaotic process possessing strong memory features. Particularly, the informational parameter $\delta_1 = \delta_1(\nu = 0)$ is very useful for analyzing different complex systems, including the physiological subjects. For example, the appearance of strong memory in MEG signals in a patient with PSE and the transition from the chaotic to robust regime allow for detecting the cerebral cortex areas, forming the epileptic seizure at PSE.

The complex interrelation existing between the nonlinear effects and the statistical ME determines high stability in brain functioning against some negative influences. A prompt interaction between the different brain areas averts developing of the collective neurons activity, typical for the PSE. Thus, the dynamics of physiological systems are manifested in many spatial and temporal scales, and the pathological states in live systems result in the changes of these spatio-temporal structures. At present special attention is directed to the problems of distinguishing and analyzing the stochastic and regular components of the experimental time series from biological and live systems. Towards this end various methods of nonlinear physics and simulation by nonlinear oscillators, methods of fractal time series analysis , methods of detrended fluctuation analysis are used.

It is necessary to notice, that the Fourier transform is meaningful with stationary signals only. According to [28] we can take into account the effect of nonstationarity by calculation of the nonstationarity function of the various orders. Our numerical estimations have shown that nonstationarity effects appear unessential for the our calculations.

4. **Experimental data for PSE.** Now we can proceed directly to the analysis of the experimental data: MEG signals recorded in a group of nine healthy human subjects and in a patient with (PSE) [25]. PSE is a common type of stimulus-induced epilepsy, defined as recurrent convulsions precipitated by visual stimuli, particularly a flickering light. The diagnosis of PSE involves finding paroxysmal spikes on an EEG in response to intermittent light stimulation. To elucidate the color-dependency of PS in normal subjects, brain activities subjected to uniform chromatic flickers with whole-scalp MEG have been measured in [25]. (Further details of the MEG experiment are found in [25]). Nine right-handed healthy adults (two females, seven males; age range 22-27 years) participated voluntarily. Subjects were screened for photosensitivity and personal or family history of epilepsy. The

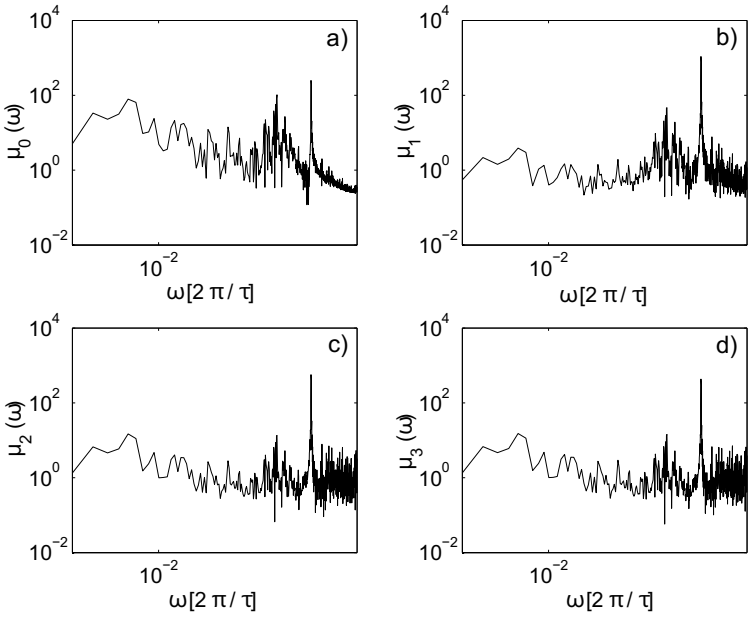


FIGURE 4. Frequency power spectra $\mu_i(\omega), i = 0, 1, 2$, and 3 for the patient with PSE (sensor No. 10) (an R/B combination of the light stimulus) for the set of the first four TCF in double log-log scale. All designations same as well as in Figure 3. One can notice noise behavior of $\mu_i(\omega)$ for $i = 0, 1, 2$, and 3.

experimental procedures followed the Declaration of Helsinki and were approved by the National Childrens Hospital in Japan.

All subjects gave their informed consent after the aim and potential risk of the experiment were explained. During the recording, the subjects sat in the magnetically shielded room and were instructed to observe visual stimuli passively without moving their eyes. Stimuli were generated by two video projectors and delivered to the viewing window in the shield room through an optical fiber bundle. Each projector continuously produced the single color stimulus. Liquid crystal shutters were located between the optical device and the projectors. By alternatively opening one of the shutters for 50 ms, 10 Hz (square-wave) chromatic flicker was produced on the viewing distance of 30 cm. Three color combinations were used: red-green (R/G), blue-green (B/G), and red-blue (R/B). CIE coordinates were x = 0.496, y = 0.396 for red; x = 0.308, y = 0.522 for green; and x = 0.153, y = 0.122 for blue. All color stimuli had a luminance of 1:6 cd/m2 in otherwise total darkness. In a single trial, the stimulus was presented for 2 s and followed by an inter trial interval of 3 s, during which no visual stimulus was displayed. In a single session, color combination was fixed.

Neuromagnetic responses were measured with a 122-channel whole-scalp neuromagnetometer (Neuromag-122; Neuromag Ltd. Finland). The Neuromag-122 has 61 sensor locations, each containing two originally oriented planner gradiometers coupled to dc-SQUID (superconducting quantum interference device) sensors. The two sensors of each location measure two orthogonal tangential derivatives of the brain magnetic field component perpendicular to the surface of the sensor array.

The planner gradiometers measure the strongest magnetic signals directly above local cortical currents. From 200 ms prior responses were analog-filtered (band-pass frequency 0.03-100 Hz) and digitized at 0.5 kHz. Eye movements and blinks were monitored by measuring an electro-oculogram. Trials with MEG amplitudes $>$ 3000fT/cm and/or electro-oculogram amplitudes $> 150\mu V$ were automatically rejected from averaging. Trials were repeated more than $>$ 80 responses then they were averaged for each color combination. The averaged MEG signals were digitally lowpass-filtered at 40 Hz, and then the DC offset during the baseline (- 100 to 0 ms) was removed. At each sensor location, the magnetic waveform amplitude was calculated as the vector sum of the orthogonal components. Peak amplitude was normalized within each subject with respect to the subject's maximum amplitude. The latency range from -100 to -1100 ms was divided with 100 ms bins. Then, the peak amplitudes were calculated by averaging all peak amplitudes within each bin.

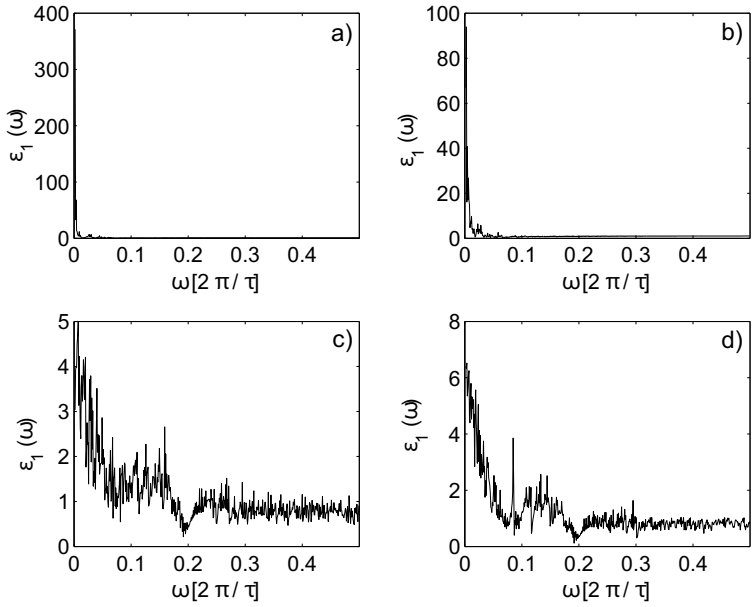


FIGURE 5. The frequency dependence in linear scale of the first point $\varepsilon_1(\omega)$ for sensor No. 10: for the healthy No. 7 (a),(b) and for patient (c),(d) an R/B (a),(c) and an R/G (b),(d) combination of the light stimulus. The emergence of the weak memory with $\varepsilon_1(\omega) >> 1$ for the healthy and strong memory with $\varepsilon_1(\omega) \sim 1$ for the patient with PSE is evident. This testifies the remarkable role of the memory in MEG signals at PSE.

5. **Results and discussions.** Typical frequency power spectra $\mu_i(\omega), i = 0, 1, 2,$ and 3 for healthy (subjects No. 7) at sensor No. 10 (Fig. 1, for usual scale and Fig. 2, for double-double scale) demonstrate fractal dependence $\mu_i(\omega) \sim \omega^{-\alpha}$ with the set of low frequency bursts. Let's remember that similar behavior is typical for the many phenomena in live systems (see for example [18, 28]). On the contrary the spectra $\mu_i(\omega)$ for the patient at sensor No. 10 (Fig. 3, for usual scale and Fig. 4, for double-double scale) show the missing of similar fractal dependence and

the appearance of the steady peak in the all spectra on the $\mu_i(\omega)$ on the specific frequency $\omega = 0.2 f.u.$

Figure 5 shows the frequency dependence of the first point $\varepsilon_1(\omega)$ for sensor No. 10: for the healthy No. 7 (a),(b) and for the patient (c),(d) an R/B (a),(c) and an R/G (b),(d) combination of the light stimulus. The emergence of the weak memory with $\varepsilon_1(\omega) >> 1$ for the healthy and strong memory with $\varepsilon_1(\omega) \sim 1$ for the patient with PSE is evident. This testifies to the remarkable role of memory in MEG signals at PSE.

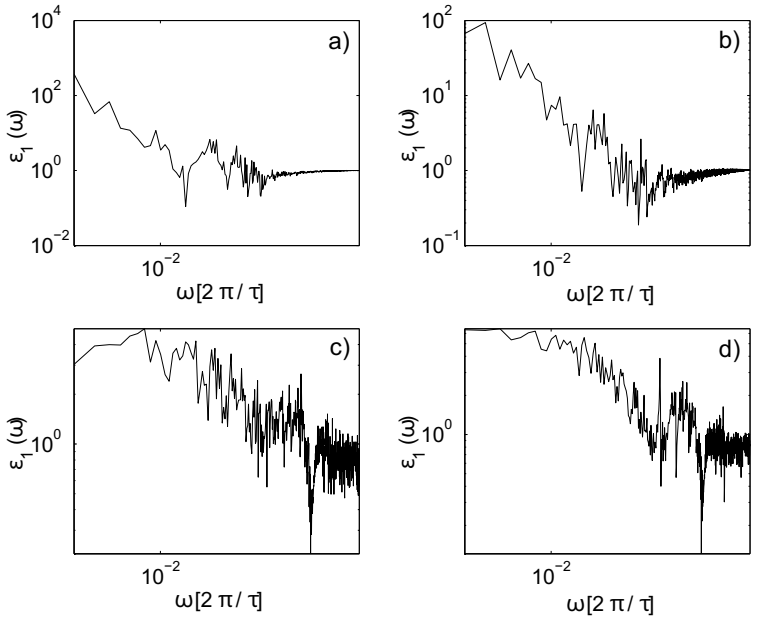


FIGURE 6. The frequency dependence of the first points $\varepsilon_1(\omega)$ for sensors No. 10: for healthy No. 7 (a),(b) and for the patient (c),(d) an R/B (a),(c) and an R/G (b),(d) combination of the light stimulus) in the double log-log scale. All designations are the same as well as in Figure 5. The drastic distinction in ME between the healthy subjects and the patient with PSE is quite apparent.

The statistical role of the ME is more prominent out of the frequency dependence of the first informational measure of memory (see Figs. 6 and 7). We observe the fractal behavior of the first memory measure $\varepsilon_1(\omega)$ for both (R/B and R/G) types of the light stimulus for healthy subjects. For the patient similar fractal behavior break-down due to the origination of the strong ME. The difference in ME for the healthy subjects versus the patient with PSE is sharper, especially for the zones of the low and superlow frequencies where long-range correlations are incorporated. Incidentally three diverse zones of fractal behavior could be found in the dependence on $\varepsilon_1(\omega)$: 1st zone for $0.7 \cdot 10^{-1} f.u. < \omega < 0.5 f.u.$, 2nd zone for $2 \cdot 10^{-2} f.u. < \omega < 0.7 \cdot 10^{-1} f.u.$ and 3rd zone for $0 < \omega < 2 \cdot 10^{-2} f.u.$, 1 f.u. $= 2\pi/\tau, \tau = 0.02 s$.

The second measure of memory $\delta_i(\omega), i = 1, 2$, and 3 describes the ME on the largest scales: Figures 7 and 8 for the healthy subjects and Figures 9 and 10 for the

patient with PSE. The difference in the ME for healthy subjects versus the patient is especially surprising at the frequency $\omega = 0$. Here this difference measures off approximately 1000 times! A similar fact arises due to the long-range correlations in the human brain neuronal activity. The crucial role of the strong memory in the stochastic dynamics of the neuromagnetic responses for the patient with PSE is particularly essential.

In drawing our conclusions about the role of the statistical memory effects we show also the averaged data for the whole group of nine healthy subjects versus the patient with PSE in Figures 11-14. The topographic dependence of the second measure of memory $\delta_1(\omega = 0; n)$ in Figure 11 (for R/B combination of the light stimulus) for healthy subjects (upper line, the data are averaged for the whole group of nine healthy subjects) versus the patient with PSE (lower line) demonstrate the striking difference in the impact of strong ME especially for the sensors with No. 5, 23, 9, 11, 14, and 23. For example, for sensor n=5 the difference acquires an approximate valuation of $10^4$ times!

To specify the role of the strong memory we introduce the spatial-topographic dependence in terms of a novel information measure, the index of memory, which is defined by:

$$\nu(n) = \delta_1^{healthy}(0; n)/\delta_1^{patient}(0; n). \tag{9}$$

This third measure quantifies the sharp revising of ME in the individual MEG sensors in the patient with PSE versus the healthy group. By means of parameter $\nu(n)$ we can try to find special zones (sensors) on the human cerebral cortex that are responsible for the mechanism of PSE. With this purpose in Figure 12 we present the topographic dependence of the information measure $\nu(n)$ for the healthy group (averaged for the whole group of nine subjects) in comparison with patient with PSE. From Figure 12 the specific role of the individual zones on the human cerebral cortex with the sensors No. 10, 5, 23 , 40 and 53 is obvious. The sharp increase of the crucial role of the ME in the stochastic behavior of the neuromagnetic signals is clearly visible for sensors with these numbers. The observed points of MEG sensors detect the areas of a protective mechanism against PSE in a the human organism: in the frontal zone (sensor n = 10), right (n = 5) and left (n = 23) temporal zones, the left parietal (n = 40) and the occipital (n = 53) zones. The early activity in these sensors may reflect the protective mechanism that suppresses cortical hyperactivity due to the chromatic flickering.

6. **Conclusions.** One can remark that some earlier steps toward understanding normal and diseased human brains have already been set in other fields of science such as neurology, clinical neurophysiology, neuroscience, and others. The numerous studies applying linear and nonlinear time series analysis to EEG and MEG in epileptic patients are discussed in detail in [25], [19], taking into account the neurophysiological basis of epilepsy, in particular PSE. Specifically, the results of [25] show that significant nonlinear structure is evident in the MEG signals for control subjects, whereas nonlinearity was not detected for the patient. In addition, the couplings between distant cortical regions were found to be greater for control subjects.

The important role of combinational chromatic sensitivity in sustained cortical excitation was also confirmed. These prior findings lead to the hypothesis that the healthy human brain is most likely equipped with significantly nonlinear neuronal

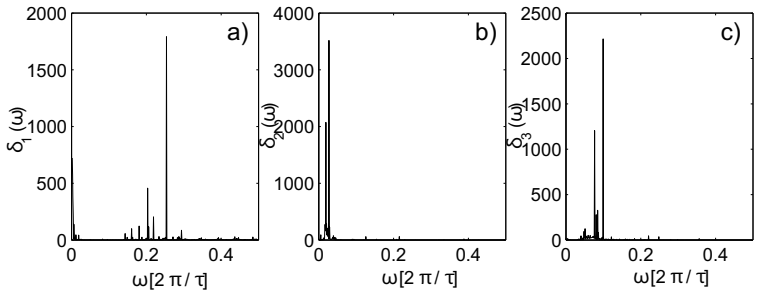


FIGURE 7. The frequency dependence in linear scale of the first three points of the second measure of memory $\delta_i(\omega)$, $i$= 1 (a), 2 (b) and 3 (c) for the healthy No. 7 (sensor No. 10) (an R/B combination of the light stimulus). One can note that the use of $\delta_i(\omega)$ amplifies the role of memory.

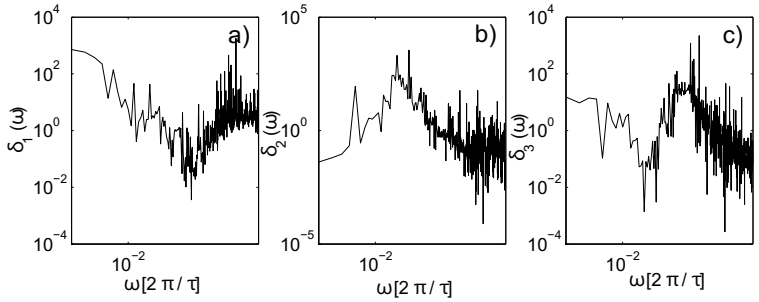


FIGURE 8. The frequency dependence of the two first points of the second measure of memory $\delta_i(\omega)$, $i$= 1 (a), 2 (b), 3 (c) for the healthy No. 7 (sensor No. 10) (an R/B combination of the light stimulus) in double log-log scale. ME are weak on the first level, and they are strong on the second and third relaxation levels.

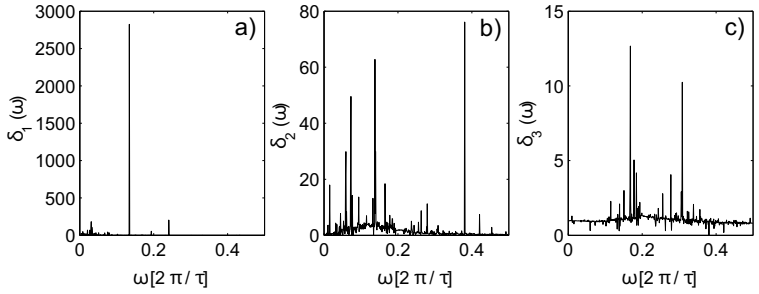


FIGURE 9. The frequency dependence in linear scale of the first three points of the second measure of memory $\delta_i(\omega)$, $i$= 1 (a), 2 (b), 3 (c) for the patient with PSE (sensor No. 10) (an R/B combination of the light stimulus). Application of parameter $\delta_i(\omega)$ allows amplifying the role of statistical memory.

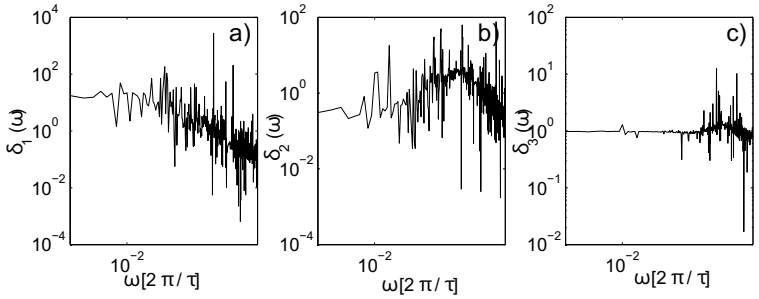


FIGURE 10. The frequency dependence of the first three points of the second measure of memory $\delta_i(\omega)$, i = 1 (a), 2 (b), 3 (c) for the patient with PSE (sensor No. 10) (an R/B combination of the light stimulus) in double log-log scale. The statistical ME in MEG's signals becomes the strongest and repeatedly reinforced.

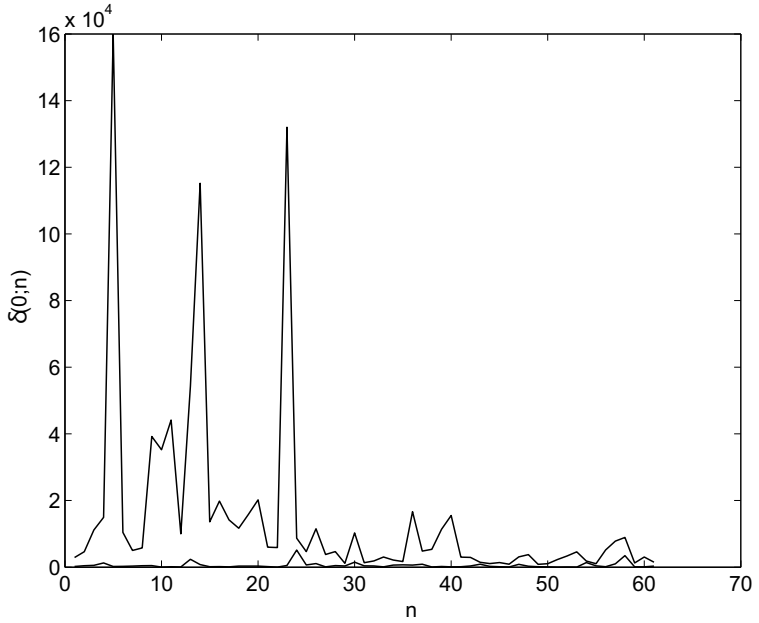


FIGURE 11. The topographic dependence of the first point in the second measure of memory $\delta_1(\omega = 0; n)$ on average for the whole group of healthy subjects (upper line) vs the patient with PSE (lower line) (for an R/B combination of the light stimulus). One can note the singular weak ME for the healthy on average in sensors with No. 5, 23, 14, 11, and 9.

processing, reflecting an inherent mechanism defending against hyper-excitation to chromatic flickering stimulus, and such nonlinear mechanism is likely to be impaired for a patient with PSE (Figs. 9, 10).

It is necessary to note that this study of chaotic behavior of the neuromagnetic signals of a human MEG'-s with PSE and in a group of the healthy subjects

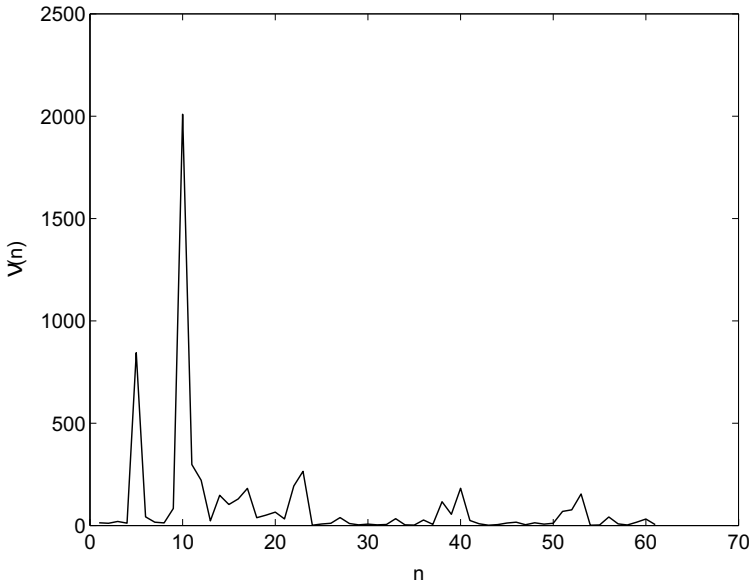


FIGURE 12. The topographic dependence of the memory index $\nu(n) = \nu_1(n;0)$ for the the whole group of the healthy subjects on average vs the patient with PSE (for an R/B combination of the light stimulus). Strong memory in the patient with PSE vs the healthy subjects appears clearly in sensors with No. 10, 5, 23, 40 and 53.

elucidates the role of statistical memory as an important criterion, measuring the functioning of the human brain. Even an insignificant amplification of the ME tests the pathological change in the brain of the patient with PSE. The pronounced sharp increases of the ME in our set of statistical quantifiers in the neuromagnetic signals indicate the pathological state of the patient with PSE within separate areas of the brain. Our approach, being conveniently constructed from the set of subordinate MF yielding the rate of change of the autocorrelation function of the measured complexity dynamics, allows one to characterize the neuromagnetic signals in the human brain in terms of statistical indicators. These so constructed statistical quantifiers in turn measure both the role and the strength of statistical memory which the underlying time series accommodate.

Many natural phenomena are described by distributions with a time scale-invariant behavior [24]. The approach suggested here allows the stochastic dynamics of neuromagnetic signals in the human brain to be treated in a probabilistic manner and to search for its statistical singularities. It is known that PSE is a type of reflexive epilepsy which originates mostly in the visual cortex (both striate and extra-striate) but with high possibility towards propagating to other cortical regions [4]. Healthy brain possibly possess an inherent controlling (or defensive) mechanism against this propagation of cortical excitations, the breakdown of which makes the brain vulnerable to trigger epileptic seizures in patients [21]. However the exact origin and dynamical nature of this putative defensive mechanism is not fully known. Earlier we showed [25] that brain responses against chromatic flickering in healthy subjects

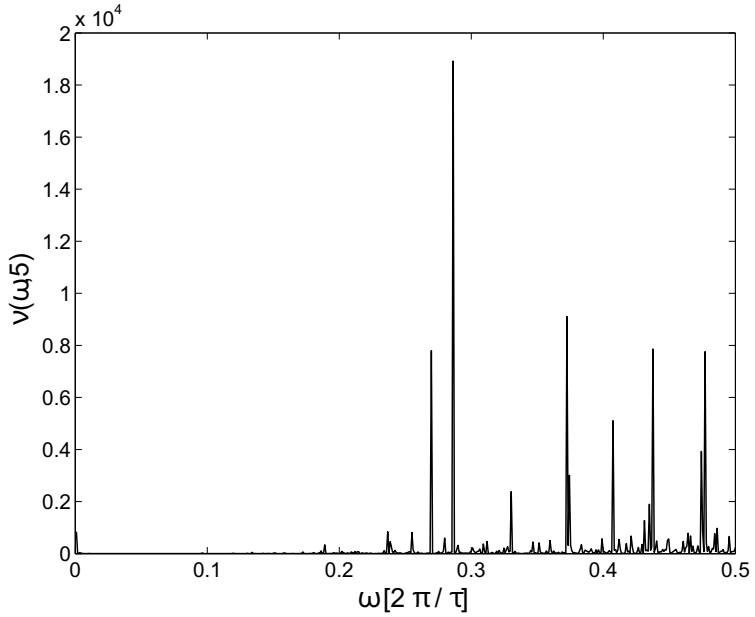


FIGURE 13. The frequency dependence of the memory index $\nu_1(\omega; 5)$ for the the whole group of healthy subjects on average vs the patient with PSE for sensor No. 5 (an R/B combination of the light stimulus). In the high frequency area one can visualize a group of high intensive bursts of the strong memory in the chaotic dynamics of neuromagnetic responses.

represent strong nonlinear structures whereas nonlinearity is dramatically reduced to minimal in patients.

Here we report that the patient's brain shows significantly stronger statistical ME than healthy brains. A complex network composed of interacting nonlinear system with memory component is inherently stable and critically robust against external perturbations. Quick inhibitory effect, that is essential for the prevention of PSE, is made possible by the faster signal processing between distant brain areas. Further, such networks are able to facilitate flexible and spontaneous transitions between many possible configurations as opposed to being entrained or locked with the external perturbations [5]. In short, our findings are in line with growing body of evidence that physiological systems generate activity fluctuations on many temporal and spatial scales and that pathological states are associated with an impairment of this spatio-temporally complex structure.

From the physical point of view the obtained results can be used as a test to identify the presence or absence of brain anomalies as they occur in a patient with PSE. The set of our quantifiers is uniquely associated with the emergence of ME in the chaotic behavior of the human cerebral cortex. The registration of the behavior of those indicators discussed here is then of beneficial use to detect pathological state of separate areas (sensors 5, 10, 23, 40, and 53) in the brain of the patient with PSE. There exist also other quantifiers of a different nature, such as the Lyapunov's exponent, Kolmogorov-Sinai entropy, correlation dimension, etc., which are widely used in nonlinear dynamics and related applications (see [13]).

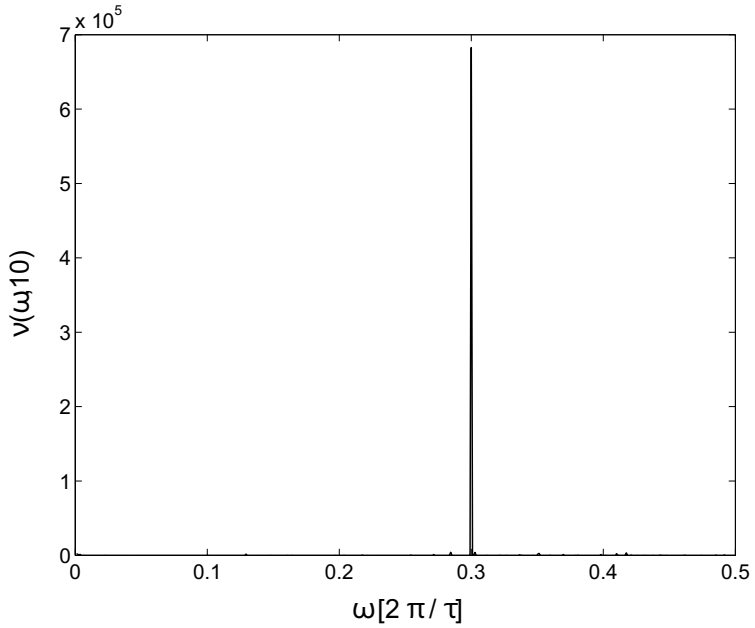


FIGURE 14. The frequency dependence of the memory index $\nu_1(\omega;10)$ for the whole group of healthy subjects on average vs the patient with PSE for sensor No. 10 (an R/B combination of the light stimulus). High peak at $\omega = 0.3f.u.$ with intensity $\nu_1(\omega;10) \sim 7\cdot 10^5$ exceeds zero frequency value $\nu_1(0;10) \sim 1.75\cdot 10^4$ approximately two orders. It means the next sharp amplification of the memory is on the frequency $\omega = 0.3f.u.$

Detailed investigations have shown that the employed memory measures are not only convenient for analysis but also ideally suited to identify anomalous brain behavior. The search for yet other quantifiers, and foremost the optimization of such measures when applied to complex, discrete time dynamics, presents a true challenge. This objective particularly holds true when attempts are made to identify and quantify an anomalous functioning in live systems. The present work presents such an initial step toward the understanding of fundamentals of physiological processes in the human brain.

**Acknowledgments.** We would like to thank the referees very much for their valuable comments and suggestions.

## REFERENCES

[1] S. Albeverio, Ph. Blanchard and L. Steil, "Stochastic processes and their Applications in Mathematics and Physics," Kluwer Academic Publ., 1990.
[2] U. Balucani, M. Lee and V. Tognetti, *Dynamical correlations*, Phys. Rep., **373** (2003), 409.
[3] V. Billock, G. de Guzman and J. Kelso, *Fractal time and 1/f spectra in dynamic images and human vision*, Physica D, **148** (2001), 136.
[4] W. A. J. Binnie C. D., in "Reflex Epilepsies and Reflex Seizures Advances in Neurology" (eds. B. Zifkin, F. Andermann, A. Beaumonir and J. Rowan), Liipincott-Raven, PA, (1998), 123.
[5] S. L. Bressler and J. A. S. Kelso, *Cortical coordination dynamics and cognition*, Trends in Cognitive Sciences, **5** (2001), 26.

[6] D. Chandler, "Introduction to Modern Statistical Mechanics," Oxford University Press, Oxford, 1987.
[7] S. Chapman and T. G. Couling, "The Mathematical Theory of Nonuniform Gases," Cambridge University Press, Cambridge, 1958.
[8] A. L. Fetter and J. D. Walecka, "Quantum Theory of Many-Particle Physics (paperback)," McGraw-Hill, New York, 1971.
[9] V. L. Ginzburg and E. Andryushin, "Superconductivity," World Scientific Publ., 2004.
[10] H. Grabert, P. Hänggi and P. Talkner, *A remark on truncation schemes of cumulant hierarchies*, J. Stat. Phys., **22** (1980), 537.
[11] M. Hämäläinen, R. Hari, P. J. Ilmoniemi, J. K. Uutila and O. V. Lounasmaa, *Magnetoencephalography-theory, instrumentation, and applications to noninvasive studies of the working human brain*, Rev. Mod. Phys., **65** (1993), 413.
[12] T. Jiang, A. Luo, X. Lia and F. Kruggel, *Comparative study of global optimization approaches to meg source localization*, Intern. J. Computer Math., **80** (2003), 305.
[13] H. Kantz and T. Schreiber, *Nonlinear time series analysis*, Cambridge Science Series, Cambridge University Press, Cambridge **7** (2000), 370.
[14] R. Kubo, *The fluctuation-dissipation theorem*, Rep. Progr. Phys., **29** (1966), 255.
[15] R. Kubo, M. Toda, N. Hashitsume and N. Saito, *Statistical physics II: Nonequilibrium statistical mechanics*, Springer Series in Solid-State Sciences, **31** (2003), 279.
[16] J. Malmivuo and R. Plonsey, "Bioelectromagnetism, Principles and Applications of Bioelectric and Biomagnetic Fields," Oxford University Press, New York, 1995.
[17] A. A. Markov, *Extension of the law of large numbers to dependent quantities*, Phys. - Math. Soc. Kazan University, **15** (1906), 135, in Russian.
[18] A. Mokshin, R. M. Yulmetyev and P. Hanggi, *Simple measure of memory for dynamical processes described by a generalized Langevin equation*, Phys. Rev. Lett., **95** (2005), 200601; New J. Phys., **7** (2005), 9.
[19] J. Parra, S. N. Kalitzin, J. Iriarte , W. Blanes, D. N. Velis and F. H. Lopes da Silva, *Gamma-band phase clustering and photosensitivity: is there an underlying mechanism common to photosensitive epilepsy and visual perception?*, Brain, **126** (2003), 1164.
[20] C. - K. Peng, S. V. Buldyrev, S. Havlin , M. Simons, H. E. Stanley and A. L. Goldberger, *Mosaic organization of DNA nucleotides*, Phys. Rev. E, **49** (1994), 1685.
[21] V. Porciatti, P. Bonanni, A. Fiorentini, et al., *Lack of cortical contrast gain control in human photosensitive epilepsy*, Nature Neuroscience, **3** (2000), 259.
[22] S. A. Rice and P. Gray, "The Statistical Mechanics of Simple Liquids," Interscience Publ. New York, 1965.
[23] I. Sachs, S. Sen and J. Sexton, "Elements of Statistical Mechanics," Cambridge University Press, Cambridge, 2006.
[24] H. Stanley, *Phase transitions: Power laws and universality*, Nature, **378** (1995), 554.
[25] K. Watanabe, T. Imada, K. Nihei and S. Shimojo, *Nonlinear dynamics of evoked neuromagentic responses signifies potential defensive mechanisms against photosensitivity*, Neuroreport, **13** (2002), 1.
[26] F. Wolf, *Symmetry, multistability, and long-range interactions in brain development*, Phys. Rev. Lett., **95** (2005), 208701.
[27] G. A. Worrell, S. D. Craunstoun, J. Echauz and B. Litt, *TEvidence for self-organized criticality in human epileptic hippocampus*, NeoroReport, **13** (2002), 2017.
[28] R. M. Yulmetyev, P. Hanggi and F. Gafarov, *Quantification of heart rate variability by discrete nonstationary non-Markov stochastic processes*, Phys. Rev. E, **65** (2002), 046107.
[29] R. Zwanzig, *Memory effects in irreversible thermodynamics*, Phys. Rev., **124** (1961), 983.
[30] R. Zwanzig, "Nonequilibrium Statistical Mechanics," Cambridge University Press, Cambridge, 2001.